Research on Growth Kinetics and Growth Mechanism of Natural Gas Hydrates in Water-in-Asphaltene-Resin-Paraffin Deposits (ARPD) and Water-in-Oil Emulsions

E. YU. SHITZ[1], V. V. KORYAKINA[2], I. K. IVANOVA[2,3], M. E. SEMENOV[2]

[1]*Republican Research Scientific-Consulting Centre for Expertise,
Moscow, Russia*

E-mail: l.u.shitz@mail.ru

[2]*Institute for Petroleum and Gas Problems, Siberian Branch, Russian Academy of Sciences,
Yakutsk, Russia*

E-mail: koryakinavv@ipng.ysn.ru

[3]*M. K. Ammosov North-Eastern Federal University,
Yakutsk, Russia*

E-mail: iva-izavella@yandex.ru

Abstract

The paper presents the results of research on natural gas hydrates in water-in-oil and water-in-asphaltene-resin-paraffin deposits (ARPD) emulsions that were carried out at the laboratory of technogenic gas hydrates of the Institute of Oil and Gas Problems, SB RAS (Yakutsk). Kinetic aspects of the hydrate formation process in the selected emulsion media, the predominant mechanisms of hydrate crystals formation, and the effect of the medium on the morphology of the growing hydrates are described in detail. Peculiarities of the growth of gas hydrates were investigated using differential scanning calorimetry (DSC) and also the synthesis technique in special high-pressure chambers.

Keywords: gas hydrates, natural gas, oil emulsion, asphaltene-resin-paraffin deposits, ARPD emulsion, hydrate formation, kinetics, mechanism, DSC

INTRODUCTION

Gas hydrates are supramolecular host-guest compounds, wherein the hydrate framework is formed by water molecules, and gas-hydrate species are placed in cavities of this frame [1]. The detailed information on the structure and properties of gas hydrates can be found in [1–3].

Nowadays, one of the main areas of gas hydrates research is the issue of prevention and combat with their formation during natural gas and oil production [4–6]. Thus, for example, the primary understanding of the mecha- nism for the formation of hydrate suspensions is considered in [6. 7]. Apart from combating hydrate plugs, hydrate formation processes in oil emulsions are suggested to be used for combined transportation along oil and associated petroleum gas pipelines as suspended hydrate particles [8, 9]. For example, as demonstrated in [10, 11], the size of the formed hydrate particles is almost equal to the dimensions of the initial drops of oil emulsions, which eliminates their coalescence during hydrate formation and makes it possible to produce gas hydrates suspended in oil.

Lately, the DSC method is widely used to explore hydrate formation in water emulsions in oils [12−17]. As demonstrated in reference [12], equilibrium conditions of hydrate formation in oil suspensions correspond to those for bulk phases, however, a large surface of the contact of water − a hydrating agent solution in oil ensures a high rate of hydrate formation. Hydrate formation from water emulsions in model muds was experimentally investigated in papers [13, 14] and an assumption was given that each of the drops in the emulsion presented an independent microreactor, what and ensured the symmetric shape of the DSC signal.

Furthermore, it was also demonstrated that according to the shape of exothermic effects, one might judge on the dispersion of the freezing phase. Thus, an asymmetric exothermic peak with a sharp beginning and an expanded completion is typical for freezing the continuous phase. A large number of small exothermic suggest freezing large drops of the disperse phase. The exothermic peaks similar to the Gaussian curve in shape are typical for freezing samples of finely dispersed emulsions, in which the freezing of each drop proceeds independently from other drops. The authors of [15] found that the greater the asymmetry of the exothermic DSC peak was, the greater was the trend of hydrate particles towards agglomeration in the investigated water-in-oil emulsion.

Thus, as demonstrated by literature analysis on this issue, both abroad [10−17] and in Russia [18, 19], most of the DSC experiments of hydrate formation in water-oil emulsions deal with the investigation of the formation of hydrates of simple gases, for example, methane., In practice, the investigation of hydrate formation from complex gas mixtures in emulsion systems, such as oil/water and ARPD/water has not been carried out.

Our paper presents research results of the kinetics and mechanisms of formation of natural gas hydrates in oil emulsions and asphaltene-resin-paraffin deposits (ARPD). The research is a continuation of the earlier published works [20, 21].

EXPERIMENTAL

Natural gas hydrates produced in inverted oil emulsions were research objects. Oil with a density of 0.855 g/cm^3 from the Irelyakhskoye oil-gas field of the Republic of Sakha (Yakutia,

Russia) containing 1.47 mass % of paraffins, 0.45 mass % of asphaltenes, 12.5 mass % of resins and ARPD of the same deposit with the average composition (20.0 mass % of paraffins, 4.1 mass % of asphaltenes, 12.6 mass % of resins, and 3.7 mass % of mechanical impurities, with a density of 0.882 g/cm^3) was used as an organic phase.

The emulsions were produced by the mechanical mixing of oil or ARPD with a mass fraction of water of 20, 40, 60, and 80 mass % without the addition of any synthetic surfactants using a rotary stirrer with a free rate of the rotation of the blades of 11000 rpm for 30 min. In such a manner, compositions of water-in-oil emulsions of 80/20, 60/40, 40/60, and 20/80 for oil/water, and 60/40, 40/60, and 20/80 for ARPD/water were received. A composition 20/80 for ARPD/water was not received because of the impossibility of complete mixing organic and aqueous components, as the maximum possible ratio of masses yielding a homogeneous and stable emulsion was reached already in a composition of ARPD/water of 40/60.

As a gas-hydrating agent, there was used natural gas from the Srednevilyuy gas condensate field of the Republic of Sakha (Yakutia) with a composition, vol. %: CH_4 92.87, C_2H_6 5.25, C_3H_8 1.21, i-C_4H_{10} 0.12, n-C_4H_{10} 0.12, N_2 0.38, CO_2 0.05.

In order to investigate phase transformations proceeding during cooling and subsequent heating, the high-pressure differential scanning calorimeter 204 HP Phoenix (Netzsch) was used. Samples of emulsions with a mass of 30 mg were loaded into steel crucibles with perforated caps. The formation and decomposition kinetics of natural gas hydrates in emulsions was analyzed in the following temperature mode: a temperature range of −22...+25 °C, natural gas pressure of 50 atm, a rate of cooling of 0.15 °C/min, of heating of 0.2 °C/min, and the temperature measurement error of ±0.1°.

Curves of degrees of water transformation into hydrate-containing phase or the process of melting hydrates α(t) (Fig. 1) were plotted by the acquired signals of phase transitions in DSC thermograms according to the expression:

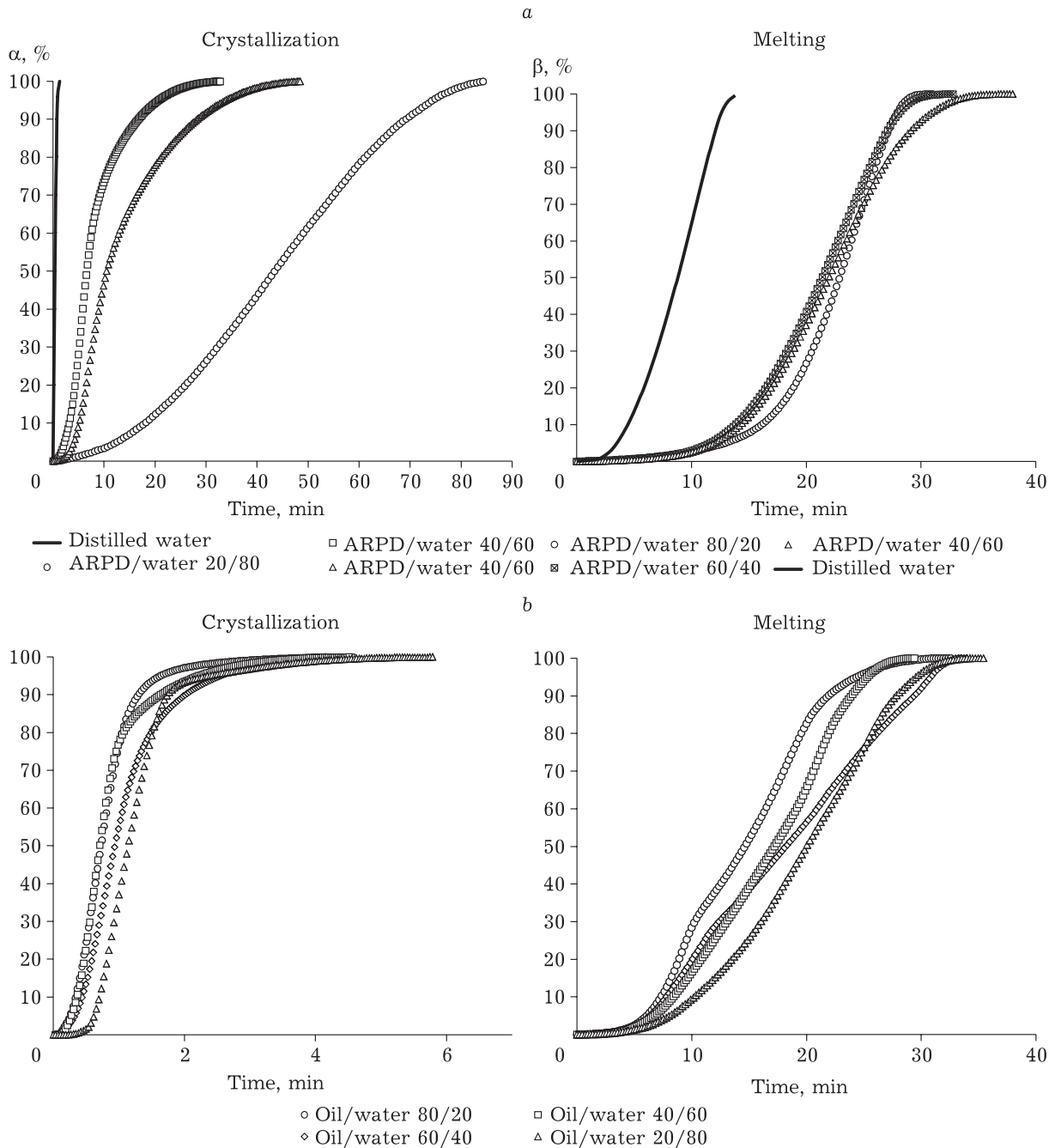$$\alpha(t) = \frac{\int_{t_0}^{t}\left(\frac{dH}{dt}\right)dt}{\int_{t_0}^{t_\infty}\left(\frac{dH}{dt}\right)dt}$$

Fig. 1. Kinetic curves of transformation degrees during crystallization (α) and melting (β) in water-in-paraffin (a) and water-in-oil (b) emulsions.

where H is the heat released during crystallization (melting) by time t; t_0 is crystallization (melting) beginning time; t_∞ is the total duration of the crystallization process.

The curves of transformation degrees (α) generated in such a way were processed according to the Erofeev − Kolmogorov − Avrami equation, by which kinetic parameters of the crystallization process of emulsion systems and the melting of hydrates were computed [22]:

$$-\ln(1 - \alpha) = kt^n$$

where k is the rate constant of crystallization (melting), n is the Avrami parameter characterising the predominant mechanism of the crystallization process.

Reference [23] demonstrates an opportunity to use the Avrami equation under nonisothermal experiment conditions in the description of the crystallization process at its early stages, with transformation degrees ranging from 0.05 to 0.7.
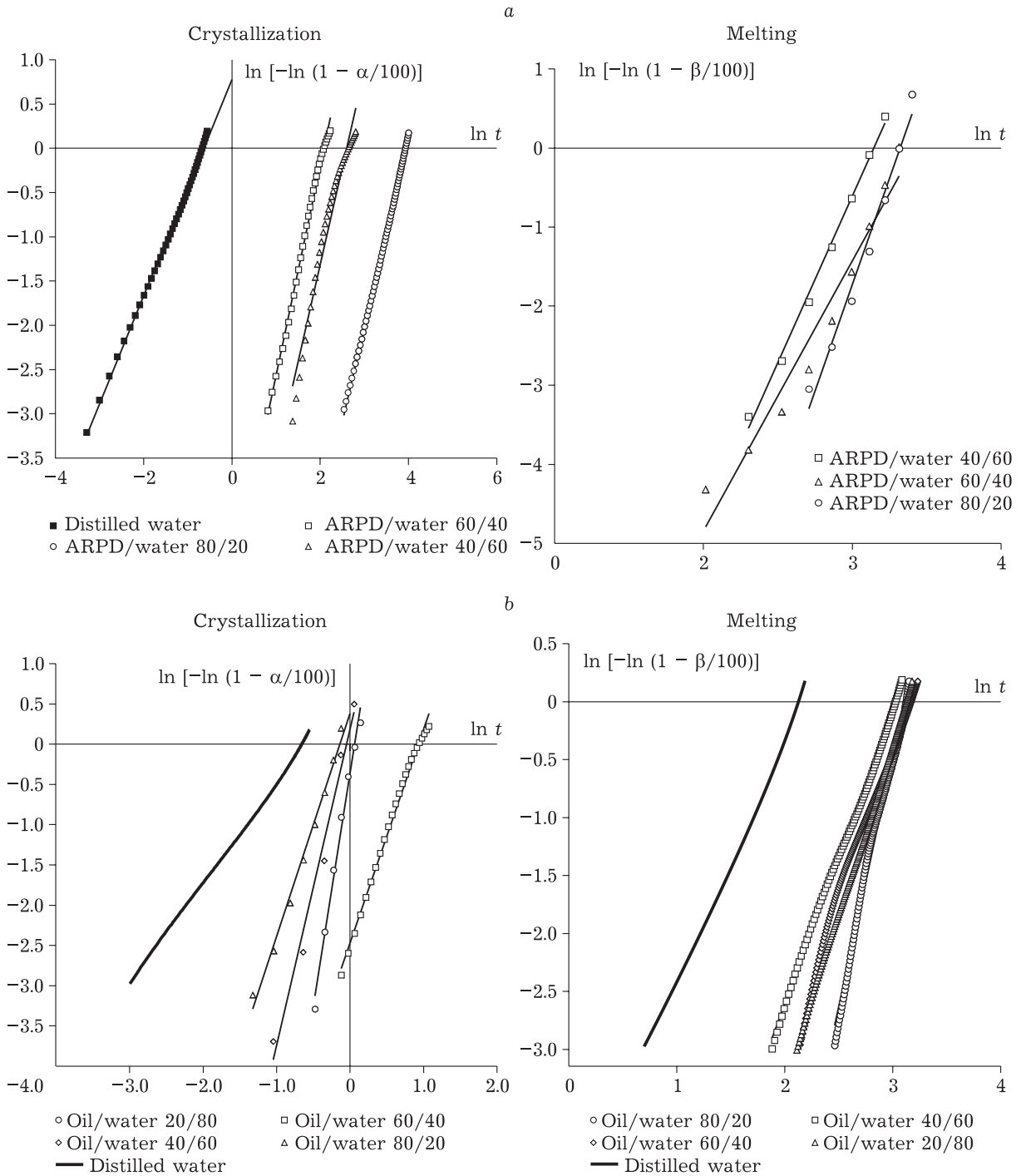
Fig. 2. Logarithmic anamorphoses of transformation degree curves during crystallization (α) and melting (β) in water-in-paraffin (*a*) and water-in-oil (*b*) emulsions.

Figure 2 presents the resulting logarithmic anamorphoses of kinetic curves in the coordinates $\ln[-\ln(1-\alpha)] - \ln t$. It can be seen that the anamorphoses are straightened in the investigated area of transformation degree values, and thus, the validity of the application of the Avrami equation for these experimental conditions has been proven.

The true rate constant of the process K (min^{-1}) was found by the Sakovich formula according to [24]:
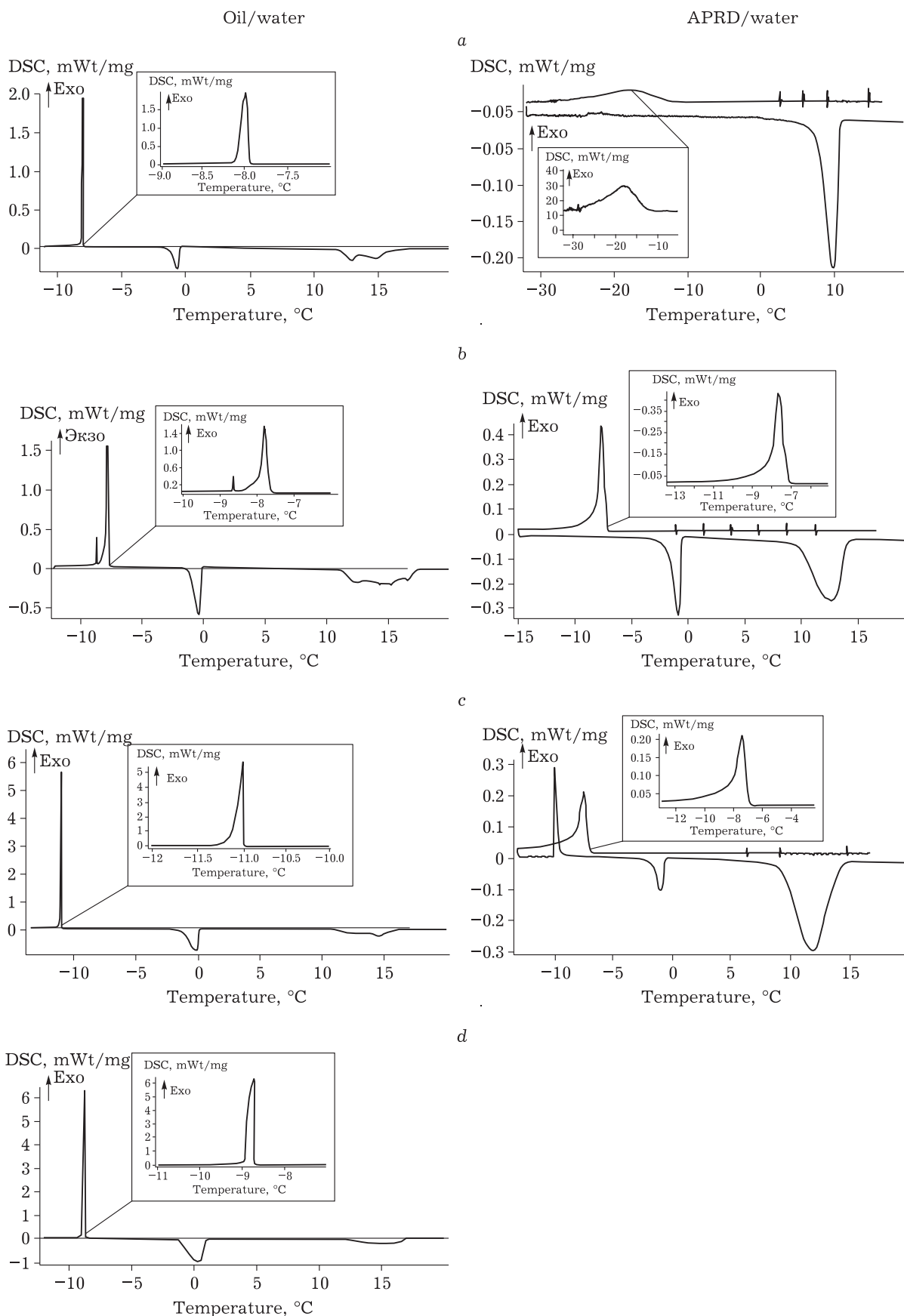
$$K_i = nk^{1/n}$$

Fig. 3. DSC thermograms of samples of oil and ARPD emulsions with different water content: 80/20 (*a*), 60/40 (*b*), 40/60 (*c*), 20/80 (*d*).

ilar fashion, as with oil emulsions: in the emulsion with a composition of paraffin/water 80/20, water crystallization peak has a very gentle curve of Gaussian shape, and the process takes place independently in each drop, and in the ARPD/water 60/40 composition, the peak is already asymmetric, in other words, a portion of water droplets are crystallized into a continuous phase and in the paraffin/water 40/60 emulsions, the peak has a very sharp beginning. Moreover, the crystallization process in this sample proceeds both during cooling and heating the emulsion.

Relying on the analysis of the resulting DSC thermograms of emulsions, kinetic parameters of processes of the formation of a hydrate-containing mixture in oil and ARPD emulsions were computed. Table 1 presents them. For comparison, the table also gives the results of the analysis of the crystallization process of natural gas hydrates in distilled water. It was found that crystallization processes the aqueous phase in both emulsions and distilled water had parameter values $n > 1$. Thus, phase transformations in emulsions proceed in the kinetic region. It can be seen that the values of the parameter ncr for oil emulsions are 1.6−2.6 times higher, and are 1.4−1.9 times greater in ARPD ones compared to those for distilled water. It was found that with increasing water content of the emulsions, the ncr parameter increased, which was probably due to an increase in degrees of freedom of the crystallization process and the acquisition of additional flow paths by it − with the transition from the microreactor mechanism of crystallization of the aqueous phase to the relay one. Thus, it was demonstrated that formation processes of natural gas hydrate in oil emulsions proceeded

along a more complex path than in distilled water, and also with increasing water content, their mechanism became more complicated.

As demonstrated by calculations, the crystallization rate (K_{cr}) of hydrates in oil emulsions is on average 15 times higher than in ARPD ones, which is related to a denser and more viscous consistency of the ARPD emulsion compared to liquid oil emulsion. As demonstrated, K_{cr} of oil emulsions decreases with crystallization temperature increasing (Fig. 4). This fact is in agreement with paper [13] that determined that an increase in overcooling oil emulsion determined as a difference between equilibrium temperature of hydrate formation and system crystallization temperature observed in the DSC experiment causes formation rate increase for methane hydrates.

Table 2 presents DSC analysis results for melting rates of natural gas hydrates in oil and ARPD emulsions.

It was determined that melting rates of hydrates acquired in the emulsions was 2−2.5 times lower than those synthesized in distilled water. It was found that hydrates in ARPD emulsions decomposed with about the same rate, regardless of the emulsion composition.

Furthermore, their stability is close to hydrates growing in oil/water 60/40 and 40/60 emulsions. As can be seen from Table 2 data, decomposition constants of gas hydrates acquired in oil emulsions reduce with water fraction increase in emulsion composition. Just to name a few, for the hydrate synthesized from the emulsion of composition 80/20, the melting rate (MR) is 2 times higher than such for the hydrate obtained from the emulsion of composition 20/80. In such a way, hydrates derived from highly watered oil emulsions are decomposed

TABLE 1

Kinetic parameters of crystallization processes of natural gas hydrates in different composition emulsions (n is process mechanism indicator; K_{cr} is crystallization rate constant, R^2 is approximation accuracy value

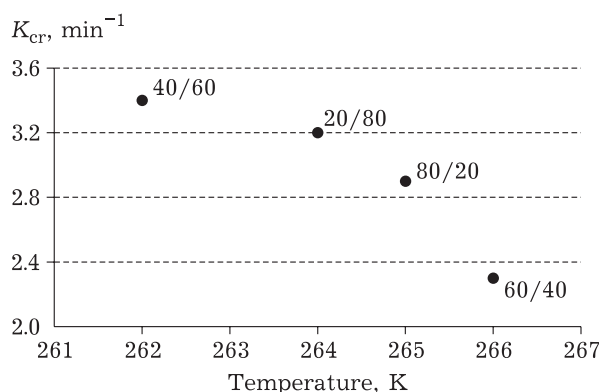| Ratio of phases organic phase/water | Organic phase type | | | | | |
| | Oil | | | ARPD | | |
	n_{cr}	K_{cr}, min^{-1}	R^2	n_{cr}	K_{cr}, min^{-1}	R^2
80/20	2.5	2.9	0.998	2.1	0.04	0.999
60/40	2.5	2.3	0.999	2.5	0.32	0.996
40/60	2.7	3.4	0.997	2.8	0.24	0.992
20/80	3.9	3.2	0.984	−	−	−

K_{cr}, min^{-1}

Fig. 4. Crystallization rate constants (K_{cr}) of natural gas hydrates in oil emulsions versus crystallization temperature.

In order to explore the morphology of natural gas hydrates growing in emulsion media, synthesis of aged emulsion samples was carried out using the original installation described in [25]. For that purpose, the emulsion sample weighing 30 g was placed in a 0.5 L polypropylene container that was loaded into a high-pressure steel cell. After sealing, the cell was vacuumed and pumped with natural gas to a pressure of 75 atm. The synthesis was carried out in a mode similar to that used in DSC analysis of emulsion samples and described in detail in [26].

RESULTS AND DISCUSSION

Figure 3 presents the thermograms of the formation of natural gas hydrates in oil/water and ARD/water samples. All the thermograms consist of two segments: one segment of cooling and the other one of heating with producing formation exotherms and melting endotherms of the hydrate.

It can be seen that thermograms of samples of emulsion systems, except for the ARPD/water 80/20 system are of similar nature. Thus, when the samples are cooled, there is an asymmetric effect of water crystallization into hydrate-containing phase, and two endothermic effects that are ice melting and hydrate decomposition are recorded in melting endotherms. There is no peak of ice melting in the ARPD/water 80/20 sample, which evidences that natural gas hydrate is formed from liquid water when cooling this emulsion.

It was found that the exothermic peak in all samples of oil/water emulsions was a sum various crystallization peaks with one common base stand. The shape of this peak has an asymmetry that increases with increasing water portion in emulsion composition. It can be seen that the crystallization peak of the oil emulsion sample with a composition of oil/water 20/80 has a sharp beginning and an extended end, which is typical for the heat effect of freezing the continuous phase. It was determined that with a decrease in the water content in the emulsion, the asymmetry of the crystallization peak decreases, and was minimum in the oil/water 80/20 emulsion sample. This suggests the freezing of mostly fine emulsion, in which crystallization of each drop of water occurs independently from each other. Thus, in oil and water emulsions, the crystallization process takes place at low water content independently on each drop of water individually − in microreactors, or, at high water content − as in a continuous phase, according to the relay type.

It was determined that depending on aqueous phase content, the crystallization process of ARPD/water emulsions proceeded in a sim-

TABLE 2

Melting rates of natural gas hydrates in different composition emulsions and distilled water

Organic phase/water ratio	Organic phase type			
	Oil		ARPD	
	MR, min^{-1}	R^2	MR, min^{-1}	R^2
80/20	0.28	0.999	0.16	0.998
60/40	0.16	0.991	0.18	0.999
40/60	0.16	0.996	0.18	0.999
20/80	0.12	0.999	−	−

Note. MR is the melting rate; R^2 is approximation accuracy value.

slower and therefore their stability is higher. Apparently, increasing the stability of hydrates may be due to changes in the dispersibility of the forming hydrates from different water content emulsions. Finely dispersed low-melting hydrates are generated in low water content emulsions, whereas hydrate agglomerates that decompose more slowly grow in highly watered emulsions. On the other hand, this is driven by the difference in the density of oil emulsions. For example, emulsions with high water contents are characterised by a viscous, dense texture, which reduces the efficiency of heat-mass-exchange during hydrate decomposition. In such a

way, as demonstrated in [27], the most stable water-in-oil emulsions are those of chocolate mousse type, of specific emulsion-gel structures and water contents of about 80–85 mass %.

In order to explore morphological peculiarities of natural gas hydrates growing in emulsion systems, their synthesis was carried out in high pressure chamber cells. Figure 4 presents photos of the resulting natural gas hydrates in the emulsion systems under study.

It can be seen that hydrates in oil emulsions are generated along the whole volume of the liquid oil phase (Table 3). When the water content is high, hydrates agglomerate and form
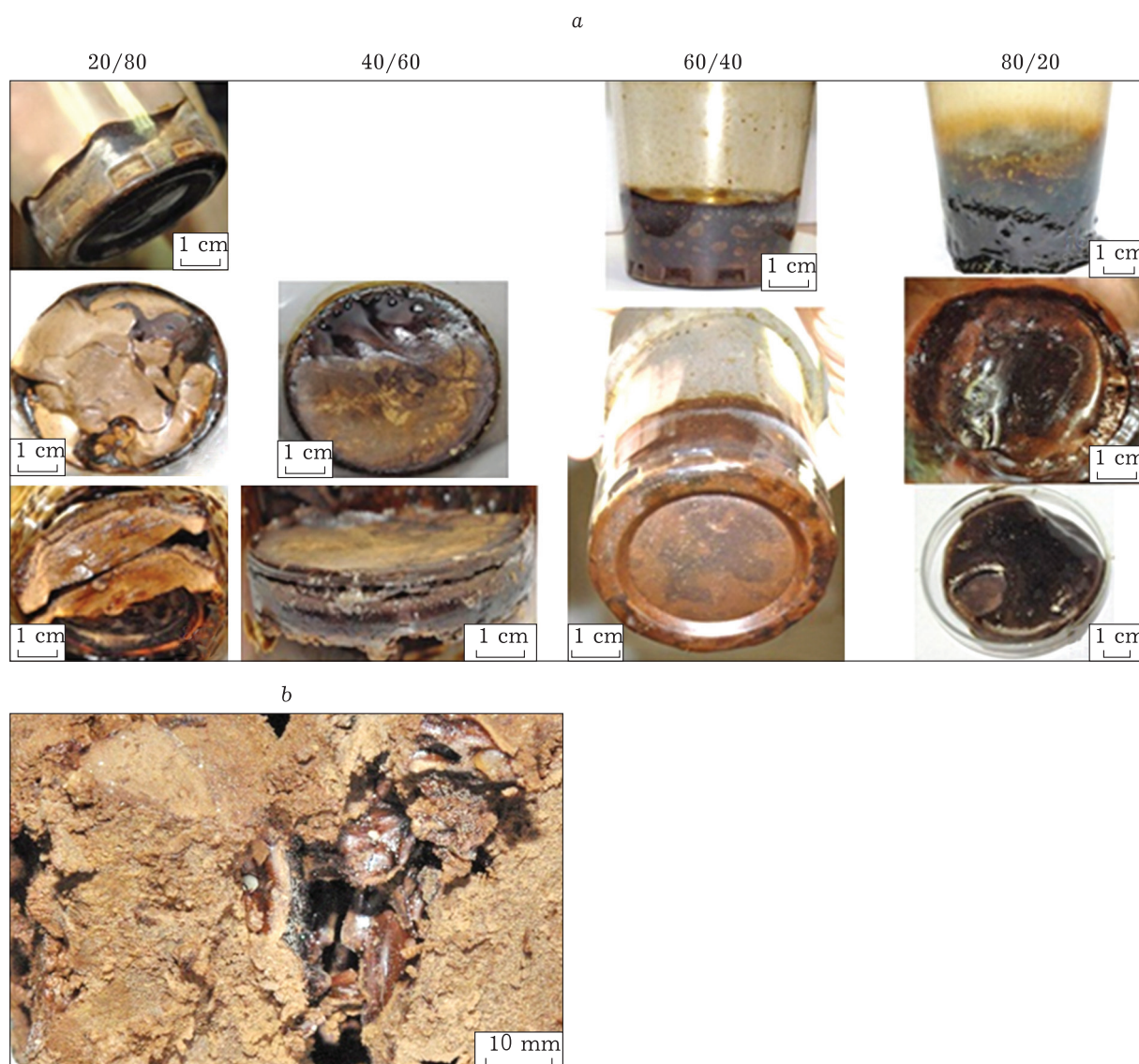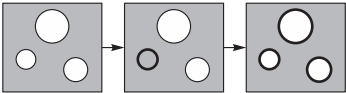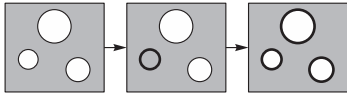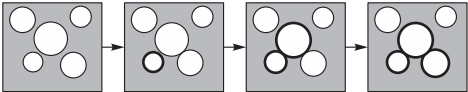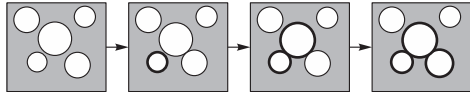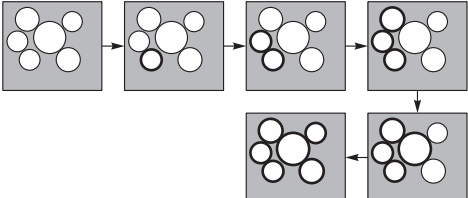

Fig. 5. Graphic images of samples of natural gas hydrates in oil emulsions (*a*) and ARPD (*b*) taken in a high-pressure cell.

TABLE 3

Suggested mechanism of hydrate formation in the medium of oil/water and ARPD/water emulsions with different water content degrees

Oil/water	ARPD/water
I. With water content of less than 40 mass %	

Micro-reactor mechanism − simple ($n_{cr} = 2.5$) proceeding at a low rate ($K_{cr} = 2.3–2.9$ min^{-1}), producing formation of low-melting hydrates (MR = 0.28 min^{-1})

Micro-reactor " mechanism − simple ($n_{cr} = 2.1$), proceeding with a very low rate ($K_{cr} = 0.4$ min^{-1}), producing formation of medium stability hydrates (MR = 0.16 min^{-1})

II. With water content 40−60 mass %

Mixed mechanism ($n_{cr} = 2.7$, $K_{cr} = 2.9–3.2$ min^{-1})

Mixed mechanism ($n_{cr} = 2.5–2.8$; $K_{cr} = 0.24–0.32$ min^{-1}), with formation of hydrates of medium stability (MR = 0.18 min^{-1})

III. With water content over 80 mass %

Relay mechanism − complicated ($n_{cr} = 3.9$), proceeding at a high rate ($K_{cr} = 3.2–3.4$ min^{-1}) with formation of stable agglomerates (MR = 0.12 min^{-1})

−

layered structures, from which hydrophobic oil is pushed. Hydrates in ARPD emulsions are generated as dispersed particles uniformly distributed in the mass of sediments due to the limitation of the free displacement because of dense emulsion consistency and large drop-shaped fragments probably resulting from uneven mixing the emulsion.

Thus, the consistency and density of the latter have an effect on the morphology of hydrates growing in emulsions. Furthermore, hydrates in oil emulsions agglomerate into large structures, whereas in dense ARPD emulsions with a rigid structure hydrate species are produced in the whole volume not sticking together among themselves.

CONCLUSION

Thus, relying on the performed research, one may suggest a probable proximate mechanism of formation of hydrate particles in oil/water and ARPD/water emulsions.

In this manner, the route of relay transfer of the crystallization procedure is added to the microreactor mechanism of crystallization of water drops, whereas the main technique of hydrate particle nucleation in ARPD emulsions is of individual nature and relay motion is not implemented due to the dense rigid structure of the ARPD emulsion.

Acknowledgements

REFERENCES

1 Sloan E. D., Koh C. A., Clathrate Hydrates of Natural Gases. London - New York: CRC Press, Boca Rator, 2008. 752 p.

2 Bik S. Sh., Gas Hydrates, Moscow: Chemistry, 1980. 296 p.

3 Sum A. K., Koh C. A., Sloan E. D., Clathrate hydrates: from laboratory science to engineering practice, *Ind. Eng. Chem. Res.*, 2009, Vol. 48, No.16, P. 7457−7465.

4 Sloan E. D., Hydrate Engineering; Vol. 21, Doherty series, Ed. by Ben Bloys Richardson, Texas: SPE H.L., 2000. 89 p.

5 Zerpa L. E., Salager J.-L., Koh C. A., Sloan E. D., Sum A. K., Surface chemistry and gas hydrates in flow assurance, *Ind. Eng. Chem. Res.*, 2011, Vol. 50, No.1, P. 188−197.

6 Sum A. K., Koh C. A., Sloan E. D., Developing a comprehensive understanding and model of hydrate in multiphase flow: From laboratory measurements to field applications, *Energy & Fuels*, 2012, Vol. 26, No. 7, P. 4046−4052.

7 Creek J. L., Efficient hydrate plug prevention, *Energy & Fuels*, 2012, Vol. 26, No.7, P. 4112−4116.

8 Pat. USA 20090124520 A1, 2009.

9 Moradpour H., Chapoy A., Tohidi B., Transportability of hydrate particles at high water cut systems and optimization of anti-agglomerant concentration, Proc. 7th International Conference on Gas Hydrates (ICGH 2011), Edinburgh, Scotland, United Kingdom, July 17-21, 2011.

10 Leba H., Cameirao A., Herri J.-M., Darbouret M., Peytavy J.-L., Gle'nat P., Chord length distributions measurements during crystallization and agglomeration of gas hydrate in a water-in-oil emulsion: simulation and experimentation, *Chem. Eng. Sci.*, 2010, Vol. 65, No. 3, P. 1185−1200.

11 Dalmazzone D., Kharrat M., Lachet V., Fouconnier B., Clausse D., DSC and PVT measurements - methane and trichlorofluoromethane hydrate dissociation equilibria, *J Thermal Analysis and Calorimetry*, 2002, Vol. 70, No. 2, P. 493−505.

12 Dalmazzone D., Hamed N., Dalmazzone C., Rousseau L., Application of high pressure DSC to the kinetics of formation of methane hydrate in water-in-oil emulsion, *J. Thermal Analysis and Calorimetry*, 2006, Vol. 85, No. 2, P. 361−368.

13 Dalmazzone D., Hamed N., Dalmazzone C., DSC measurements and modulation of the kinetics of methane hydrate formation in water-in-oil emulsion, *Chemical Engineering Science*, 2009, Vol. 64, No. 9, P. 2020−2026.

14 Dalmazzone C., Noik C., Clausse D., Application of DSC for emulsified system characterization, *Oil & Gas Science and Technology*, *Rev. IFP*, 2009, Vol. 64, No. 5, P. 543−555.

15 Colombel E., Gateau P., Barre L., Gruy F., Palermo T., Discussion of agglomeration mechanisms between hydrate particles in water-in-oil emulsions, *Oil & Gas Science and Technology*, *Rev. IFP*, 2009, Vol. 64, No. 5. P. 629−636.

16 Clausse D., Gomez F., Dalmazzone C., Noik C. A., Method for the characterization of emulsions, thermogranulometry: Application to water-in-crude oil emulsions, *J. Colloid. Interface Sci.*, 2005, Vol. 287, No. 2, P. 694−703.

17 Davies S. R., Hester K. C., Lachance J. W., Koh C. A., Sloan E. D., Studies of hydrate nucleation with high pressure differential scanning calorimetry, *Chem. Eng. Sci.*, 2009, Vol. 64, No. 2, P. 370−375.

18 Stoporev A. S., Manakov A. Yu., Kosyakov V. I., Shestakov V. A., Altunina L. K., Strelets L. A., Nucleation of methane hydrate in water-in-oil emulsions: role of the phase boundary, *Energy & Fuels*, 2016, Vol. 30, No. 5, P. 3735−3741.

19 Semenov M. E., Manakov A. Yu., Shitz E. Yu., Stoporev A. S., Altunina L. K., Strelets L. K., Misyura S. Ya., Nakoryakov V. E., DSC and thermal imaging studies of methane hydrate formation and dissociation in water emulsions in crude oils, *J. of Thermal Analysis and Calorimetry*, 2015, Vol. 119, No. 1, P. 757−767.

20 Ivanova I. K., Koryakina V. V., Semenov M. E., Rozhin I. I., *Acta Chemica Iasi*, 2016, Vol. 24, No. 2, P. 139−157.

21 Ivanova I. K., Semenov M. E., Koryakina V. V., Shits E. Yu., Rozhin I. I., *Rus. J. Appl. Chem.*, 2015, Vol. 88, No. 6. P. 941−948.

22 Avrami M. Kinetics of Phase Change, *J. Chem. Phys.*, 1939, Vol. 7, P. 1103−1112.

23 Kuo M. C., Huang J. C., Chen M., Non-isothermal crystallization of kinetic behavior of alumina nanoparticle filled poly (ether ether ketone), *Materials Chemistry and Physics*, 2006, Vol. 99, No. 2−3, P. 258−268.

24 Rozhovsky A.Yu., Kinetics of Topochemical Reactions, M.: Chemistry, 1974.

25 Semenov M. E., Kalacheva L. P., Shits E. Yu., Rozhin I. I., Natural gas hydrate decomposition in the presence of methanol, *Chemistry for Sustainable Development*, 2010, Vol. 18, P. 147−151.

26 Koryakina V. V., Ivanova I. K., Shits E. Yu., Synthesis of natural gas hydrates in inverse oil emulsions, *Chemistry for Sustainable Development*, 2017, Vol. 25, No. 6, P. 633−638.

27 Evdokimov I. N., Eliseev N. Yu., Iktisanov V. A., J. *Colloid and Interface Science*, 2005, Vol. 285, No. 2, P. 795−803.